

A Mini Review of Recent Advances in Optical Pressure Sensor

Gihun Lee^{1,*}, Hyunjin Kim^{1,*}, and Inkyu Park^{1,+}

Abstract

Innovative and advanced technologies, including robots, augmented reality, virtual reality, the Internet of Things, and wearable medical equipment, have largely emerged as a result of the rapid evolution of modern society. For these applications, pressure monitoring is essential and pressure sensors have attracted considerable interest. To improve the sensor performance, several new designs of pressure sensors have been researched based on resistive, capacitive, piezoelectric, optical, and triboelectric types. In particular, optical pressure sensors have been actively studied owing to their advantages, such as robustness to noise and remote sensing capability. Herein, a review of recent research on optical pressure sensors with self-powered sensing, remote sensing, high spatial resolution, and multimodal sensing capabilities is presented from the viewpoints of design, fabrication, and signal processing.

Keywords: Optical pressure sensors, Self-powered sensors, Remote sensing, Multimodal sensing, Spatial resolution

1. INTRODUCTION

With the rapid evolution of high-tech industries, innovative and disruptive technologies such as robotics, augmented reality (AR), virtual reality (VR), the Internet of Things (IoT), and wearable healthcare devices have emerged in recent years. Pressure monitoring is crucial for these applications in the form of electronic skin, human-machine interfaces, and physiological signal monitoring devices. For instance, tactile feedback from a pressure sensor is essential for the ability of a robot to delicately manipulate fragile objects [1]. In addition, flexible tactile sensors are in the spotlight as wearable control interfaces between humans and machines and have been actively demonstrated by many researchers [2].

Various pressure sensors have been investigated for better performance based on diverse transduction principles, including resistive, capacitive, piezoelectric, optical, and triboelectric types. These sensors can convert mechanical stimuli into a variety of electrical signals such as resistance, capacitance, and voltage. Capacitive-type pressure sensors are widely used owing to their

simple structure and sensitivity. For example, Yang et al. developed a capacitive-type pressure sensor with high sensitivity based on a sandwiched structure composed of an electrode-porous pyramid dielectric layer-electrode [3]. When pressure is applied to the sensor, the dielectric layer is compressed, and the distance between the electrodes attached to the layer decreases, leading to an increase in capacitance. However, the capacitance method may be susceptible to noise such as an external electric field, resulting in inaccurate measurements. Piezoresistive pressure sensors have high sensitivity and require fewer electronics and is therefore simple to make and integrate [4]. However, piezoresistive sensors are affected by ambient temperature because of the resistivity dependence on temperature and exhibit relatively high hysteresis and long-term stability issues compared to capacitive-type pressure sensors.

Compared to the abovementioned methods, optical pressure sensors have unique advantages. They are immune to electronic noise [5]. In addition, they allow remote pressure sensing, that is, the pressure applied at a certain location can be remotely measured. Remote sensing is useful in harsh environments with high temperatures and humidity. Additionally, rich information can be extracted from the light, such as intensity and spectrogram by photodiodes, spectrometers, and cameras. Imaging pressure distribution with high spatial resolution can be achieved by decoding the complex information of light with advanced signal processing methods, including neural-network-based calibration methods. In addition, research on multimodal sensing, such as pressure, strain, and temperature, based on optical transduction

¹Department of Mechanical Engineering, Korea Advanced Institute of Science and Technology (KAIST), Daejeon, 34141, South Korea

⁺Corresponding author: inkyu@kaist.ac.kr

*These authors equally contributed to this work

(Received: Jan. 19, 2023, Revised: Jan. 25, 2023, Accepted: Jan. 30, 2023)

This is an Open Access article distributed under the terms of the Creative Commons Attribution Non-Commercial License (<https://creativecommons.org/licenses/by-nc/3.0/>) which permits unrestricted non-commercial use, distribution, and reproduction in any medium, provided the original work is properly cited.

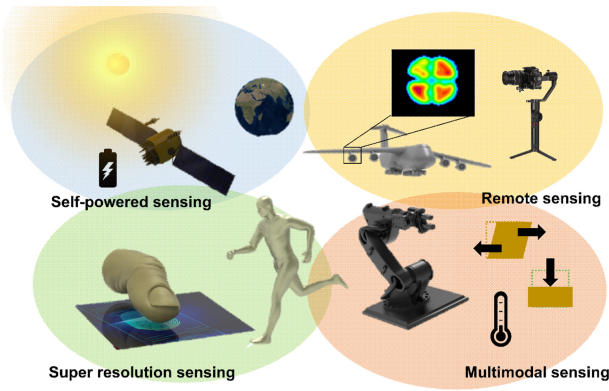


Fig. 1. Overview of recent research trends of optical pressure sensors: self-powered sensing, remote sensing, super-resolution sensing, and multimodal sensing.

mechanisms is being actively conducted. Typical structures of optical pressure sensors comprise a light source, medium, and photodetector, in which case the power is consumed by the light source and photodetector. Recently, self-powered optical pressure sensors have been actively researched adapting solar cells and ambient light instead of photodetectors and light sources.

This paper introduces recently developed optical pressure sensors used for remote sensing, multimodal sensing, high spatial resolution performance, and self-powering ability from various perspectives, including design, fabrication, and signal processing, as shown in Fig. 1.

2. SELF-POWERED OPTICAL PRESSURE SENSOR

The optical pressure sensor system consists of three components: light source, media, and detector. Recently, research on optical pressure sensors for realizing self-powered devices by eliminating the power consumption of the source has been actively conducted. Among self-powered optical pressure sensors in which a light source is provided by the system itself, interest in a mechanoluminescent (ML) system based on light emission induced by friction or mechanical deformation is increasing. For example, a composite of zinc sulfide (ZnS) particles and polydimethylsiloxane (PDMS) is widely used in sensor applications that require repeatability and a long lifetime because light is generated during elastic deformation [6]. ZnS:Cu²⁺/Mn²⁺ (595 nm), ZnS:Cu²⁺ (525 nm), and ZnS:Cu⁺ (475 nm) emit orange, green, and blue light, respectively. It has the advantage of being able to design a multichannel system because it can generate light in various wavelength bands by appropriately

combining particles. Hou et al. designed a mouthguard system using the aforementioned principle (Fig. 2(a)) [7]. At each position on the mouthguard, the light of different colors emitted by pressure passes through a common optical fiber to reach a single RGB sensor. The generated light behavior for various mouth movements was measured using two RGB sensors and processed using machine learning. As shown in Fig. 2(b), Zhang et al. proposed a self-powered multimodal sensor system to measure bending and stretching behaviors using a ZnS:Cu particle-PDMS composite and to measure pressure via triboelectric signals generated from silver nanowires and PDMS [8]. Wang et al. demonstrated a triboelectric nanogenerator (TENG) sensor and an ML (ZnS:Mn) sensor integrated to enable measurements over a wide pressure range [9]. However, the systems introduced in these two studies have some drawbacks. A complex circuit is required to measure the TENG signal, and the ML structure requires a fairly large pressure owing to the high limit of detection. To overcome these limitations, Su et al. proposed a pressure sensor in which ML and photoluminescence (PL) materials were fused (Fig. 2(c)) [10]. The proposed structure consisted of a PL layer with (Sr,Ca) SiAlN₃:E²⁺ and a triboelectrification-induced electroluminescence (TIEL) layer with ZnS:Cu. The TIEL layer is a source for emitting green light, and the PL layer, which is made of a porous structure, works as a color-conversion layer. In the low-pressure regime, red light is induced by red-converted green light from the TIEL layer. As the pressure increased, the color conversion performance of the compressed PL layer decreased, and the green light emitted from the ZnS:Cu of the TIEL layer became predominant (peak wavelength of the emitted light changed from 650 to 510 nm with pressure). The self-powered device demonstrated that it could measure a wide range of pressures (0.01 – 2.4MPa) using only an optical signal. To improve the sensor characteristics, such as resolution and limit of detection, studies on increasing the wavelength change according to the ML pressure and brightness of the emitted light should be continuously performed.

In Fig. 2(d), a self-powered optical pressure sensor using ambient light as the source was proposed by Choi et al. [11]. The pores in the porous structure made of Ecoflex generate a large amount of light scattering, which increases the effective light path length and reduces the amount of light reaching the detector. When the pores are closed by pressure, the intensity of the light reaching the detector becomes relatively large. A self-powered optical pressure sensor that operates under ambient light conditions was implemented by applying two organic solar cells for calibration. While most of the TENG-based self-powered

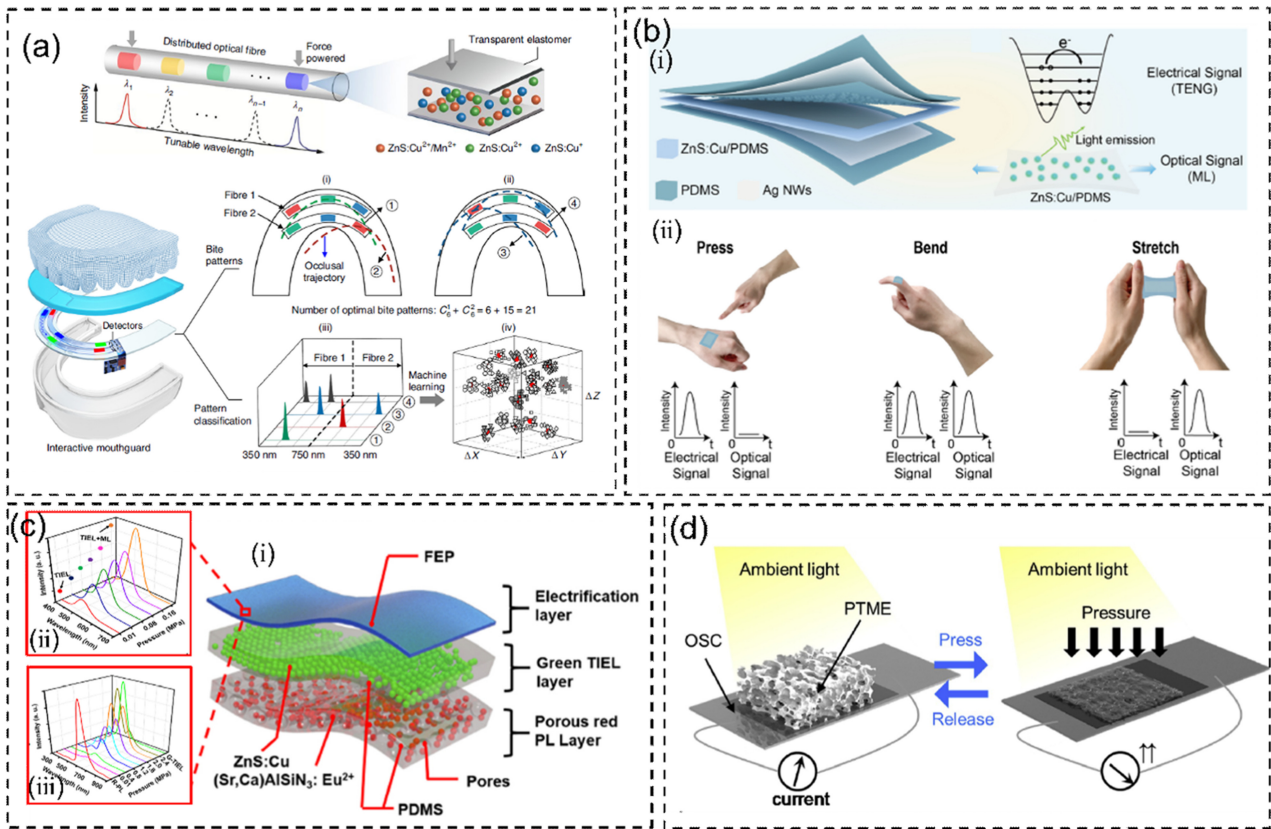


Fig. 2. Self-powered optical pressure sensors. (a) Schematic diagram of a mouth guard system in which a single RGB sensor detects lights of different color from mechanoluminescent (ML) blocks. ML blocks are made from a mixture of ZnS:Cu²⁺/Mn²⁺, ZnS:Cu²⁺, and ZnS:Cu⁺ particles Ref. [7] Copyright (2022) Springer Nature Limited. (b) Schematic illustration of a system (i) that measures physical behaviors (ii) through electrical signals (triboelectric nanogenerator (TENG) based sensor) and optical signals from ML material Ref. [8] Copyright (2022) Elsevier (c) A system configuration of the optical pressure sensor in which the color of the emitted light varies according to the pressure (i). ZnS:Cu is a triboelectrification-induced electroluminescence (TIEL) material that emits brighter green light (510 nm) when pressure is applied (ii). The porous PL layer behaves as a color filter that changes green light to red light (650 nm) (iii). When the pores are closed by pressure, the filter performance is weakened, making higher green light intensity Ref. [10] Copyright (2020) Elsevier. (d) A conceptual diagram of the operation of an optical pressure sensor system in which an organic solar cell and porous structure are applied. When pressure is applied, the light transmittance increases, and a higher current is generated Ref. [11] Copyright (2020) Elsevier.

sensing methods introduced above are limited to dynamic pressure measurement, this system can measure static pressure.

3. REMOTE SENSING

Remote sensing is one of the most important features of an optical pressure sensor system and its advantages are as follows. First, it is possible to acquire data from a long distance in harsh environments, such as high blast pressure or high temperature, thus ensuring the safety of the sensor system. In particular, it is unnecessary to consider the temperature and humidity stability of the electronic components because the pressure information is transmitted through light. Second, a simple system configuration using a commercial camera is possible. Typical electrical sensors

require complex systems such as amplifiers, analog-digital-converters, micro-controller units, and wireless communication modules. However, in most optical pressure sensors, components other than the detector do not require complex circuits. Finally, a system configuration that does not require power is possible. For TENGs, components for signal amplification and data processing are essential. However, optical pressure sensors visualize pressure as light intensity or color, allowing the human eye to estimate the intensity or distribution of pressure without using complicated measurement setups.

The detector for an optical pressure sensor system generally consists of a photoelectric conversion element that converts light energy into an electrical signal and can be applied in various ways, from photodetectors to cameras. Shi et al. measured the shear force, pressure, and temperature distribution using a camera

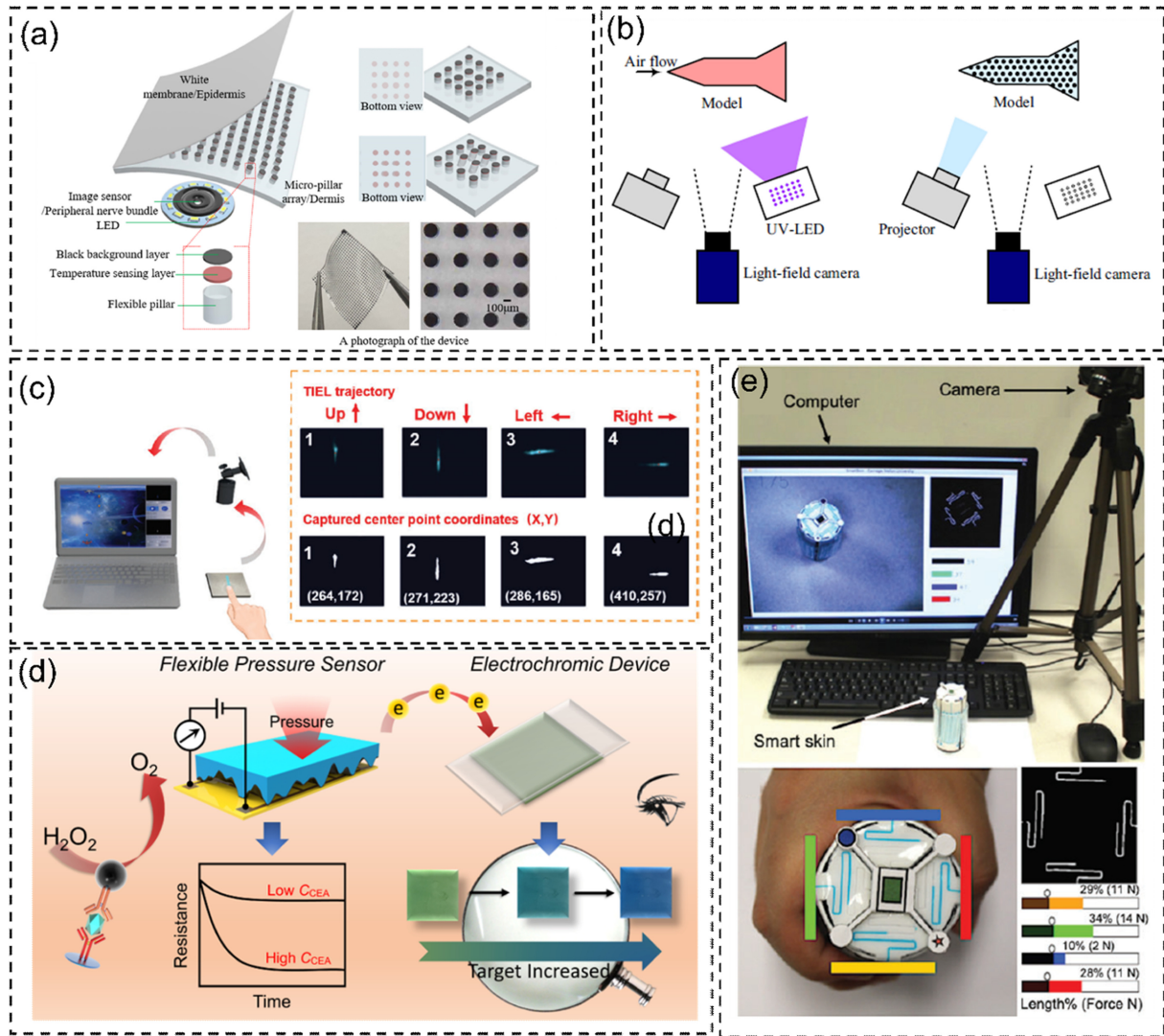


Fig. 3. Optical sensor for remote sensing. (a) Schematic illustration of the system for measuring various mechanical behaviors and temperature through a micropillar with a temperature-sensitive layer. Data is acquired through an image sensor Ref. [12] Copyright (2020) John Wiley and Sons, Inc. (b) Schematic diagram of the system with remote sensing of the pressure distribution of a fluid Ref. [13] Copyright (2018) Springer Nature Switzerland AG. (c) Schematic diagram of pressure telemetry with TIEL material. Direction information is obtained through TIEL trajectory Ref. [14] Copyright (2022) John Wiley and Sons, Inc. (d) Principle of remote pressure sensing system with integrated piezoresistive pressure sensor and electrochromic display Ref. [16] Copyright (2021) American Chemical Society. (e) Remote pressure measurement system using the principle of a pressure gauge. Depending on the pressure, the blue fluid fills the fluidic channel and the pressure is evaluated through the image Ref. [17] Copyright (2022) Mary Ann Liebert.

image sensor (Fig. 3(a)) [12]. A micropillar array structure containing a temperature liquid crystal composite (TLC) was positioned between the image sensor and source. The color of the TLC changes according to the temperature, cross-sectional area of the pillar increases with the applied pressure, and lateral deformation of the pillar due to shear is analyzed using camera images. Shi et al. presented the method to measure 3D pressure distribution of the using a light-field camera from a distance. (Fig. 3(b)) [13]. A 2D pressure distribution is obtained using pressure-sensitive paint and combine it with a textured light-field image

that provides depth map information to obtain a pressure distribution on a 3D surface. Optical pressure sensors require that there are no obstacles that interfere with light propagation between the light source and detector. Otherwise, the light is not visible because it is blocked by the object that exists between the light source and detector, or a position error may occur when measuring the pressure through the light around the object, as shown in Fig. 3(c) [14,15]. To solve this problem, the display part can be separated from the pressure sensing part. Not only an electrical connection between the sensing and display parts but

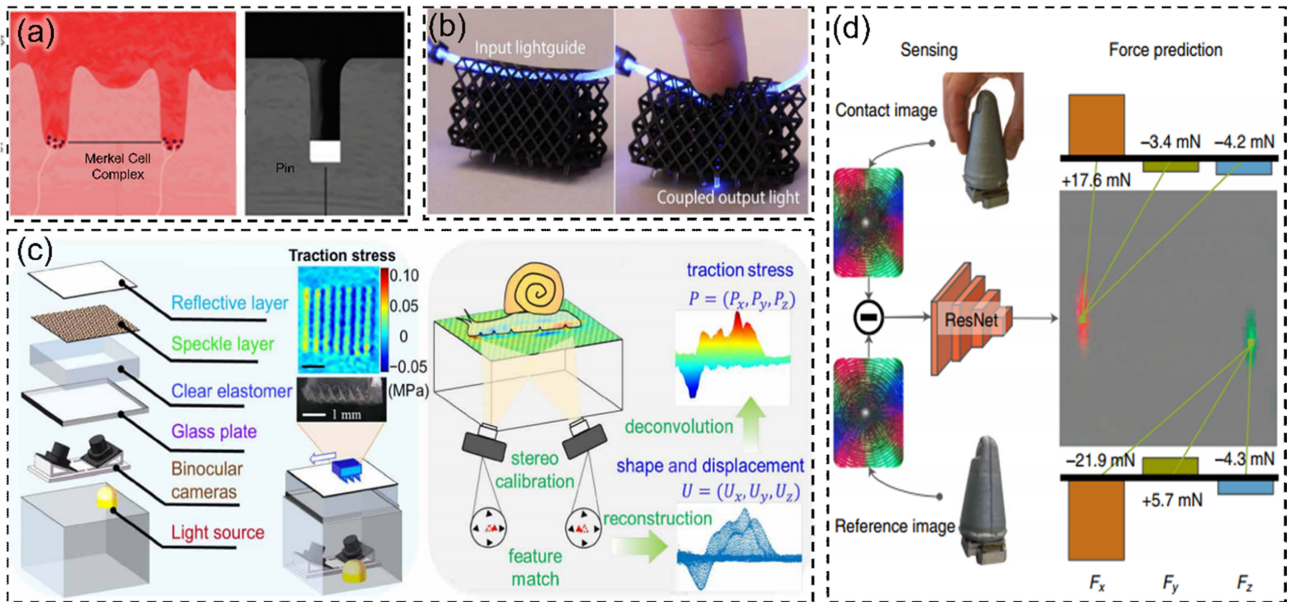


Fig. 4. Optical tactile sensors with high spatial resolution. (a) A marker inside the tactile sensor mimicking the Merkel cell inside the human fingertip Ref. [18] Copyright (2018) Mary Ann Liebert. (b) Stretchable optical fiber inside the 3D-printed polyurethane lattice Ref. [19] Copyright (2019) American Association for the Advancement of Science. (c) Multilayered structure of sensor with binocular cameras and process of obtaining the interfacial stress from the captured figures of the deformed surface Ref. [21]. Copyright (2022) American Association for the Advancement of Science. (d) Residual Neural Network (ResNet) based estimation of force map when the two fingers pinch the sensor Ref. [25] Copyright (2022) Springer Nature Limited.

also an optical connection, such as optical fibers and waveguides, allows for the accurate measurement of the pressure distribution. As shown in Fig. 3(d), Yu et al. manufactured a piezoresistive-type pressure sensor by coating a conductive polypyrrole (PPy) film on a PDMS structure with a rough surface using sandpaper as the mold [16]. As the conductivity increases with increasing pressure, the color of the electrochromic device based on polyaniline, and tungsten oxide in the display part changes (green to blue), enabling remote pressure sensing. As shown in Fig. 3(e), the remote sensing of pressure using camera images, rather than light intensity and color, was reported by Han et al. [17]. A closed microfluidic channel containing air and a blue-colored ionic liquid (1-ethyl-3-methylimidazolium ethyl sulfate) was designed, and the pressure was measured using the principle that air is compressed according to pressure, and the colored liquid fills the channel. It has the advantage of being able to measure pressure without precise calibration in ambient light environments.

4. HIGH SPATIAL RESOLUTION

Recently, tactile sensors with a high spatial resolution have been actively studied for robotic manipulation and object recognition.

Here, we introduce optical tactile sensors with design and signal-processing strategies for high-spatial-resolution pressure mapping. Fig. 4 (a) shows a skin-inspired structure with internal pins on the underside of its skin-like membrane, mimicking intermediate ridges within the human fingertip [18]. The camera inside the sensor detected deformations of the shell by visually tracking the markers, reaching the spatial resolution with submillimeter accuracy for all types of sensors they suggested. Xu et al. developed a 3D mechanosensory network cointegrated with compliant structures using stretchable optical fibers and a 3D-printed polyurethane lattice, as shown in Fig. 4(b) [19]. The sensor achieved human skin-comparable spatial resolution with the error of 0.71mm. Lee et al. fabricated a structure with a transparent piezoresistive layer in contact with a quantum dot light-emitting diode (QLED) layer to image the applied pressure [20]. The very thin structure and use of QLEDs made it possible to map high spatial resolution pressure without distortion in an analog manner, resulting high resolution pressure imaging with more than 1000 dpi. Yuanzhe et al. developed a binocular stereo-vision-based traction force microscopy method [21]. They reached spatial resolution with 100 μm over a 60 mm-by-50mm field of view. Based on stereo camera calibration, the 3D deformation of the contact surface can be well reconstructed, which is crucial for

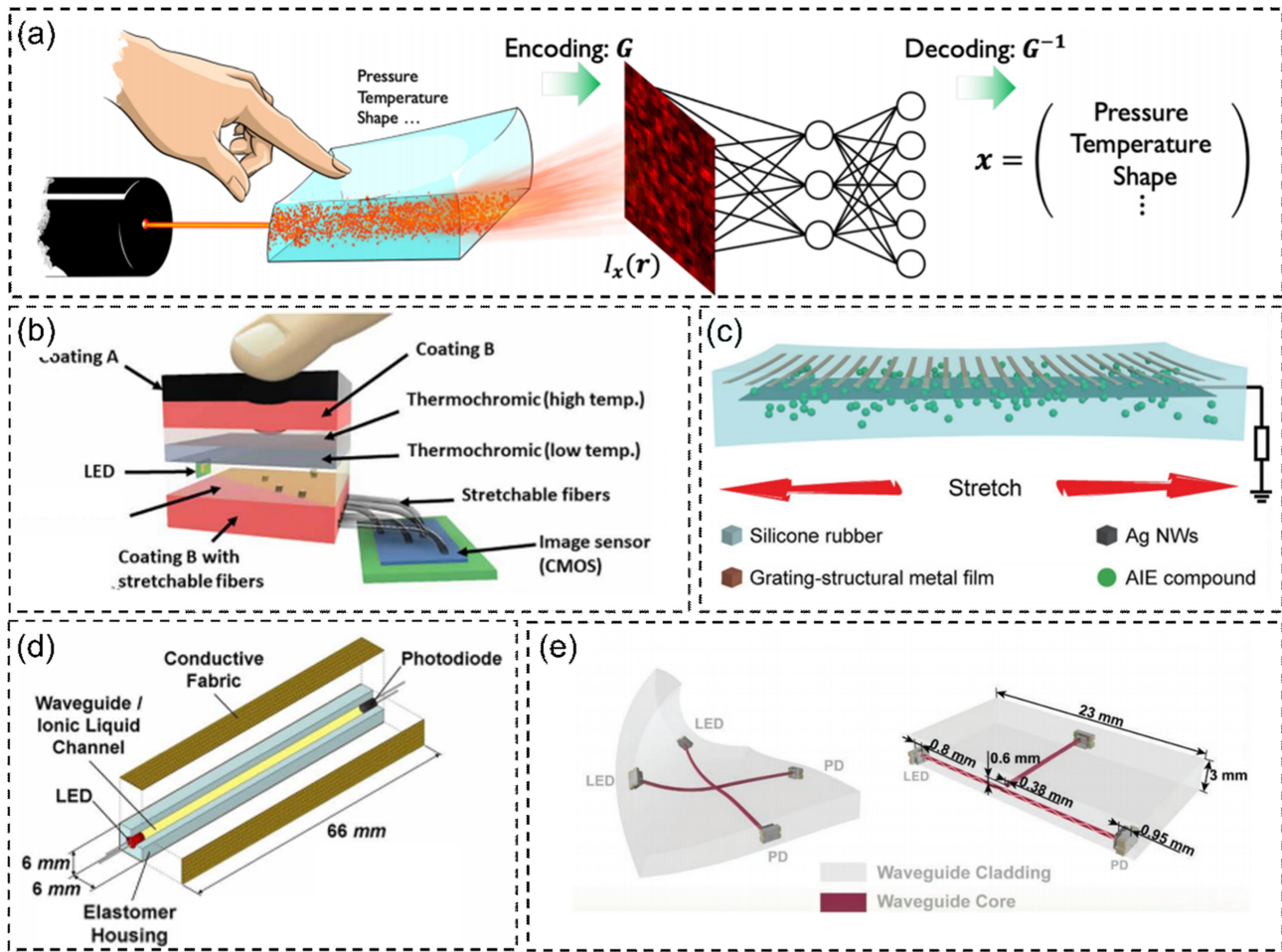


Fig. 5. Multimodal pressure sensors. (a) Conceptual schematic of signal processing of the speckle pattern Ref. [27] Copyright (2022) Springer Nature Limited. (b) Functional layers including thermochromic layers and components of the robotic flesh Ref. [28] Copyright (2022) American Association for the Advancement of Science. (c) Structure of triboelectric-photonic skin Ref. [30] Copyright (2018) John Wiley and Sons. (d) Structure of soft sensors with heterogeneous sensing mechanisms Ref. [31]. Copyright (2020) American Association for the Advancement of Science. (e) Structure of multi-axial tactile sensor with crossed-over waveguides embedded in and its cross-sectional diagram Ref. [33]. Copyright (2022) John Wiley and Sons.

estimating the traction stress (Fig. 4(c)).

In particular, machine learning techniques are actively employed to decode complex tactile information that depends on the location where the force is applied. They are applied to optical mechanism-based tactile sensors that contain information regarding the deformation of the sensing surface [22,23]. Piacenza et al. fabricated a tactile sensor attached to a finger with three layers consisting of a flexible printed circuit board layer mounting a light emitting diode (LED) and photodiode, a transparent waveguide layer, and a thin reflective layer [24]. Then, they created a multilayer perceptron (MLP) structure achieving the regression of position and force, classification of multi-touch with submillimeter force localization accuracy, and accurate determination of the normal contact force over 3D surfaces. Sun

et al. developed a similar robotic finger structure, including an elastomeric layer and reflective layer [25]. They utilized a camera, a ring-shaped LED inside the finger, and a Residual Neural Network architecture to infer the distribution of forces, achieving spatial resolution of 0.4mm. The data flow used to estimate the force map is shown in Fig. 4(d).

5. MULTIMODAL SENSING

Different multimodal sensor systems that respond to various stimuli such as pressure, strain, temperature, and humidity are crucial for stable manipulation and enhanced interaction between humans and machines. For instance, the capability of measuring

pressure and temperature simultaneously is essential for the robot hand to recognize objects, and is further applicable to garbage sorting [26]. The optical scattering phenomenon inside a soft material can be used to sense various external stimuli. Sho et al. captured the speckle pattern with a digital camera and employed a convolutional neural network (CNN)-based algorithm for decoding complex interference patterns caused by indentation depth corresponding to the pressure, temperature, and indenter position, as shown in Fig. 5(a) [27]. Temperature-dependent phenomena, such as thermal expansion/contraction and changes in the refractive index, yielded different speckle patterns. The thermochromic gel is a possible choice for capturing temperature, and the structure leveraging this material is shown in Fig. 5(b) [28]. The thermochromic layers change color with temperature, leading to a shift in the wavelength corresponding to the color change in the thermochromic gels. Also, single optical microfiber showed a potential for simultaneously sensing temperature and pressure [29]. Thermal stimulation caused larger changes in the refractive index of the core than cladding, which induced a shift of the cutoff frequency on the light spectrum, and pressure stimulation caused the bending of the core, resulting in a decrease in light intensity.

Integration with other sensing mechanisms, such as triboelectricity and piezoresistivity, has also been conducted. Bu et al. combined optical strain sensing with triboelectric pressure sensing [30]. Fig. 5(c) shows the photonic skin structure with a microcracked copper film over the aggregation-induced emission (AIE) compound and a stretchable conducting layer of Ag NW. As strain was applied, the size of the microcrack increased and the exposed AIE particles increased, resulting in increased brightness of the photonic skin. The sensor also functioned as a pressure sensor based on TENG capabilities, which responded with a high level of consistency, regardless of the applied strain. Kim et al. reported a soft sensor integrating three heterogeneous sensing mechanisms: optoelectronics, microfluidics, and piezoresistivity [31]. The sensor structure was constructed in three parts: a microfluidic channel filled with ionic liquid, an elastomer housing, and an outside conductive fabric layer, as shown in Fig. 5(d). Signal patterns from heterogeneous mechanisms appeared independent each other according to the deformation modes. And they constructed multilayer perceptron model for signal processing which consists of one input layer, three hidden layers, and one output. Since three signals are obtained from each mechanism and a total of eight modes must be distinguished (no deformation, 3 single-mode deformation, 4 multimode deformation), the input and the output layer has three nodes and eight nodes

respectively. By this method, the sensor could distinguish stretching, bending, compression, and combinations of these deformation modes (a total of seven deformation modes) with a simple fabrication process.

To interpret complex contact information for texture, shape, and slip detection, tactile sensors capable of detecting and differentiating multidirectional forces, such as shear and torsion, are crucial. Takeshita et al. developed a shear force sensor with the ability to independently measure shear forces along two axes [32]. When a shearing force is exerted on the elastic gum surface, the cylindrical bar inside the gum tilts around the hole. Consequently, the mirror was attached to the cylindrical bar tilts according to the magnitude of the shearing force. The sensor determines the tilt angle of the mirror by using an optical sensor. Zhou et al. developed a waveguide sensor that can distinguish normal and shear components from the two-dimensional vector forces [33]. The sensor comprised two waveguide cores placed at different depths and arranged in a cross-bar configuration, as shown in Fig. 5(e). Light-emitting diodes (LEDs) and photoelectric detectors are embedded at the two ends of each optical waveguide core, providing light sources and detecting light powers, respectively. Here, the anisotropic sensitivity of a single waveguide fiber to multiaxial forces was employed.

6. CONCLUSIONS

This review discusses recent research trends and performance enhancements of optical pressure sensors and confirms their potential in various applications such as wearable devices, sensors, and robotics. Optical pressure sensors can measure pressure in various ways, such as changes in intensity, color, image pattern, and remote sensing. In addition, with various efforts to achieve self-powered sensing using ML and TIEL materials, excellent spatial resolution and multimodal sensing performance have been achieved by many researchers. Nevertheless, several challenges remain for the performance enhancement of optical pressure sensor systems, and it is necessary to improve the filter performance of the detector and narrow the bandwidth of the light emitted from the source to enhance multichannel systems. Increasing the sensor resolution and detection distance by improving the quantum efficiency of the detector and the intensity of the emitted light should also be considered. In addition, a more precise pressure distribution measurement that improves the spatial resolution of the detector array is required. Owing to the low interference between channels

and the ability to transmit and receive large amounts of data, optical pressure sensors are expected to have a high demand in areas requiring multichannel and high-resolution performance, such as wearable pressure sensors and robot fingers.

ACKNOWLEDGMENT

This work was supported by the following research grants. (1) This work was supported by the Technology Innovation Program (20020292, Development of Heterogeneous Multi-Sensor Micro-System Platform) funded By the Ministry of Trade, Industry & Energy (MOTIE, Korea). (2) This work was supported by the Technology Development Program (3104117) funded by the Ministry of SMEs and Startups (MSS, Korea).

REFERENCES

- [1] H. Oh, G. C. Yi, M. Yip, and S. A. Dayeh, “Scalable tactile sensor arrays on flexible substrates with high spatiotemporal resolution enabling slip and grip for closed-loop robotics”, *Sci. Adv.*, Vol. 6, No. 46, pp. eabd7795(1)-eabd7795(14), 2020.
- [2] S. Pyo, J. Lee, K. Bae, S. Sim, and J. Kim, “Recent Progress in Flexible Tactile Sensors for Human-Interactive Systems: From Sensors to Advanced Applications”, *Adv. Mater.*, Vol. 33, No. 47, p. 2005902, 2021.
- [3] J. C. Yang, J. O. Kim, J. Oh, S. Y. Kwon, J. Y. Sim, D. W. Kim, H. B. Choi, and S. Park, “Microstructured porous pyramidal-based ultrahigh sensitive pressure sensor insensitive to strain and temperature”, *ACS Appl. Mater. & Interfaces*, Vol. 11, No. 21, pp. 19472-19480, 2019.
- [4] M. I. Tiwana, S. J. Redmond, and N. H. Lovell, “A review of tactile sensing technologies with applications in biomedical engineering”, *Sens. Actuator A Phys.*, Vol. 179, pp. 17-31, 2012.
- [5] X. Liu, I. I. Iordachita, X. He, R. H. Taylor, and J. U. Kang, “Miniature fiber-optic force sensor based on low-coherence Fabry-Perot interferometry for vitreoretinal microsurgery”, *Biomed. Opt. Express*, Vol. 3, No. 5, pp.1062-1076, 2012.
- [6] Y. Zhuang and R. J. Xie, “Mechanoluminescence rebrightening the prospects of stress sensing: a review”, *Adv. Mater.*, Vol. 33, No.50, p. 2005925, 2021.
- [7] B. Hou, L. Yi, C. Li, H. Zhao, R. Zhang, B. Zhou, and X. Liu, “An interactive mouthguard based on mechanoluminescence-powered optical fibre sensors for bite-controlled device operation”, *Nat. Electron.*, Vol. 5, No. 10, pp. 682-693, 2022.
- [8] X. Zhang, Z. Li, W. Du, Y. Zhao, W. Wang, L. Pang, L. Chen, A. Yu, and J. Zhai, “Self-powered triboelectric-mechanoluminescent electronic skin for detecting and differentiating multiple mechanical stimuli”, *Nano Energy*, Vol. 96, p. 107115, 2022.
- [9] X. Wang, M. Que, M. Chen, X. Han, X. Li, C. Pan, and Z. L. Wang, “Full dynamic-range pressure sensor matrix based on optical and electrical dual-mode sensing”, *Adv. Mater.*, Vol. 29, No. 15, p. 1605817, 2017.
- [10] L. Su, Z. Jiang, Z. Tian, H. Wang, H. Wang, and Y. Zi, “Self-powered, ultrasensitive, and high-resolution visualized flexible pressure sensor based on color-tunable triboelectrification-induced electroluminescence”, *Nano Energy*, Vol. 79, p. 105431, 2021.
- [11] J. Choi, D. Kwon, B. Kim, K. Kang, J. Gu, J. Jo, K. Na, J. Ahn, D. del Orbe, K. Kim, J. Park, J. Shim, J. Y. Lee, and I. Park, “Wearable self-powered pressure sensor by integration of piezo-transmittance microporous elastomer with organic solar cell”, *Nano Energy*, Vol. 74, p. 104749, 2020.
- [12] X. Shi, Y. Chen, H.-L. Jiang, D.-L. Yu, and X.-L. Guo, “High-Density Force and Temperature Sensing Skin Using Micropillar Array with Image Sensor”, *Adv. Intell. Syst.*, Vol. 3, No. 8, p. 2000280, 2021.
- [13] S. Shi, S. Xu, Z. Zhao, X. Niu, and M. K. Quinn, “3D surface pressure measurement with single light-field camera and pressure-sensitive paint”, *Exp. Fluids*, Vol. 59, pp. 1-10, 2018.
- [14] L. Su, Q. Xiong, H. Wang, and Y. Zi, “Porous-Structure-Promoted Tribo-Induced High-Performance Self-Powered Tactile Sensor toward Remote Human-Machine Interaction”, *Sci. Adv.*, Vol. 9, No. 32, p. 2203510, 2022.
- [15] Y. Zhuang, X. Li, F. Lin, C. Chen, Z. Wu, H. Luo, L. Jin, and R. Xie, “Visualizing Dynamic Mechanical Actions with High Sensitivity and High Resolution by Near-Distance Mechanoluminescence Imaging”, *Adv. Mater.*, Vol. 34, No. 36, p. 2202864, 2022.
- [16] Z. Yu, G. Cai, X. Liu, and D. Tang, “Pressure-based biosensor integrated with a flexible pressure sensor and an electrochromic device for visual detection”, *Anal. Chem.*, Vol. 93, No. 5, pp. 2916-2925, 2021.
- [17] Y. Han, A. Varadarajan, T. Kim, G. Zheng, K. Kitani, A. Kelliher, T. Rikakis, and Y. L. Park, “Smart Skin: Vision-Based Soft Pressure Sensing System for In-Home Hand Rehabilitation”, *Soft Robot.*, Vol. 9, No. 3, pp. 473-485, 2022.
- [18] B. Ward-Cherrier, N. Pestell, L. Cramphorn, B. Winstone, M. E. Giannaccini, J. Rossiter, and N. F. Lepora, “The tactip family: Soft optical tactile sensors with 3d-printed biomimetic morphologies”, *Soft Robot.*, Vol. 5, No. 2, pp. 216-227, 2018.
- [19] P. A. Xu, A. K. Mishra, H. Bai, C. A. Aubin, L. Zullo, and R. F. Shepherd, “Optical lace for synthetic afferent neural networks”, *Sci. Robot.*, Vol. 4, No. 34, p. eaaw6304, 2019.
- [20] B. Lee, J. Y. Oh, H. Cho, C. W. Joo, H. Yoon, S. Jeong, E. Oh, J. Byun, H. Kim, S. Lee, J. Seo, C. W. Park, S. Choi, N. M. Park, S. Y. Kang, C. S. Hwang, S. D. Ahn, J. I. Lee, and Y. Hong, “Ultraflexible and transparent electroluminescent skin for real-time and super-resolution imaging of pressure distribution”, *Nat. Commun.*, Vol. 11, No. 1, p. 663, 2020.
- [21] Y. Li, P. Bai, H. Cao, L. Li, X. Li, X. Hou, J. Fang, J. Li, Y. Meng, L. Ma, and Y. Tian, “Imaging dynamic three-dimensional traction stresses”, *Sci. Adv.*, Vol. 8, No. 11, p.

- eabm0984, 2022.
- [22] Y. Yan., Z. Hu, Z. Yang, W. Yuan, C. Song, J. Pan, and Y. Shen, “Soft magnetic skin for super-resolution tactile sensing with force self-decoupling”, *Sci. Robot.*, Vol. 6, No. 51, p. eabc8801, 2021.
- [23] H. Sun and G. Martius, “Guiding the design of super-resolution tactile skins with taxel value isolines theory”, *Sci. Robot.*, Vol. 7, No. 63, p. eabm0608, 2022.
- [24] P. Piacenza, K. Behrman, B. Schifferer, I. Kymissis, and M. Ciocarlie, “A sensorized multicurved robot finger with data-driven touch sensing via overlapping light signals”, *IEEE/ASME Trans. Mechatron.*, Vol. 25, No. 5, pp. 2416-2427, 2020.
- [25] H. Sun, K. J. Kuchenbecker, and G. Martius, “A soft thumb-sized vision-based sensor with accurate all-round force perception”, *Nat. Mach. Intell.*, Vol. 4, No. 2, pp. 135-145, 2022.
- [26] G. Li, S. Liu, L. Wang, and R. Zhu, “Skin-inspired quadruple tactile sensors integrated on a robot hand enable object recognition”, *Sci. Robot.*, Vol. 5, No. 49, p. eabc8134, 2020.
- [27] S. Shimadera, K. Kitagawa, K. Sagehashi, Y. Niiyama, T. Miyajima, and S. Sunada, “Speckle-based high-resolution multimodal soft sensing”, *Sci. Rep.*, Vol. 12, No. 1, p. 13096, 2022.
- [28] J. A. Barreiros, A. Xu, S. Pugach, N. Iyengar, G. Troxell, A. Cornwell, S. Hong, B. Selman, and R. F. Shepherd, “Haptic perception using optoelectronic robotic flesh for embodied artificially intelligent agents”, *Sci. Robot.*, Vol. 7, No. 67 p. eabi6745, 2022.
- [29] N. Yao, X. Wang, S. Ma, X. Song, S. Wang, Z. Shi, J. Pan, S. Wang, J. Xiao, and H. Liu, “Single optical microfiber enabled tactile sensor for simultaneous temperature and pressure measurement”, *Photonics Res.*, Vol. 10, No. 9, pp. 2040-2046, 2022.
- [30] T. Bu, T. Xiao, Z. Yang, G. Liu, X. Fu, J. Nie, T. Guo, Y. Pang, J. Zhao, F. Xi, C. Zhang, and Z. L. Wang, “Stretchable triboelectric–photonic smart skin for tactile and gesture sensing”, *Adv. Mat.*, Vol. 30, No. 16, p. 1800066, 2018.
- [31] T. Kim, S. Lee, T. Hong, G. Shin, T. Kim, and Y. L. Park, “Heterogeneous sensing in a multifunctional soft sensor for human-robot interfaces”, *Sci. Robot.*, Vol. 5, No. 49, p.eabc6878, 2020.
- [32] T. Takeshita, K. Harisaki, H. Ando, E. Higurashi, H. Nogami, and R. Sawada, “Development and evaluation of a two-axial shearing force sensor consisting of an optical sensor chip and elastic gum frame”, *Precis. Eng.*, Vol. 45, pp. 136-142, 2016.
- [33] J. Zhou, Q. Shao, C. Tang, F. Qiao, T. Lu, X. Li, X. Liu, and H. Zhao, “Conformable and Compact Multiaxis Tactile Sensor for Human and Robotic Grasping via Anisotropic Waveguides”, *Adv. Mat. Technol.*, Vol. 7, No. 11, p. 2200595, 2022.